Original Article

The landscape of PD-L1 expression and somatic mutations in hepatocellular carcinoma

Hao Xu, Xiao-Lu Liang, Xiao-Guang Liu, Nian-Ping Chen

Department of Hepatobiliary Surgery, Affiliated Hospital of Guangdong Medical University, Zhanjiang, China

Contributions: (I) Conception and design: XG Liu, NP Chen; (II) Administrative support: XG Liu, NP Chen; (III) Provision of study materials or patients: XL Liang; (IV) Collection and assembly of data: H Xu; (V) Data analysis and interpretation: H Xu, XL Liang; (VI) Manuscript writing: All authors; (VII) Final approval of manuscript: All authors.

Correspondence to: Xiao-Guang Liu; Nian-Ping Chen. Department of Hepatobiliary Surgery, Affiliated Hospital of Guangdong Medical University, No 57 South Renmin Avenue, Xiashan District, Zhanjiang 524001, China. Email: xiaoguanghb@hotmail.com; FSNP6688@126.com.

Background: Hepatocellular carcinoma (HCC) is the most common primary malignancy of the liver, and becoming the third-leading cause of cancer-related mortality worldwide. Despite the immune checkpoint inhibitors and molecular targeted therapies have shown preferable efficacy in HCC, large number of HCC patients do not respond effectively to anti-PD-1 reagents. Besides, the accumulation of genetic mutations in cancer cells may lead to the therapy resistant. Hence, there are clinical gaps between genetic and transcriptomic biomarkers for the HCC treatment.

Methods: To investigate the genetic mapping of liver cancer, targeted deep sequencing (TDS) and bioinformatics analysis were performed on hepatocellular carcinoma (HCC) tumor tissues and matched blood samples. Furthermore, copy number variants (CNVs) and Tumor mutation burden (TMB) were calculated. Immunohistochemistry was applied to determine the PD-L1 expression in HCC tumor tissues. Clinical characteristic, PD-L1 expression, and the TMB were analyzed in 32 HCC patients.

Results: This study indicated that the PD-L1 positive patients exhibited a lower TMB compared to the PD-L1 negative group, and PD-L1 positive patients were more likely to suffer from aggressive clinicopathologic features than PD-L1 negative patients. We also verified the top 30 mutated genes, including *TP53*, *CTNNB1*, *KMT2D*, *AXIN1*, *ALK*, and *NOTCH1*, in our dataset. Our results indicated that PD-L1 positive patients possessed more tumors with vascular invasion and advanced CCLC stage. Moreover, PD-L1 positive patients exhibited a lower TMB compared to the PD-L1 negative group.

Conclusions: These findings could improve our understanding of the effects of immune checkpoint therapies on prognosis, and could facilitate the monitoring of somatic mutations in HCC.

Keywords: PD-L1; targeted gene sequencing; hepatocellular carcinoma; tumor mutational burden (TMB); mutation landscape

Submitted Mar 18, 2021. Accepted for publication Jun 15, 2021.
doi: 10.21037/jgo-21-251
View this article at: https://dx.doi.org/10.21037/jgo-21-251

Introduction

Hepatocellular carcinoma (HCC) is the most common primary malignancy of the liver, the fifth most common cancer, and the third-leading cause of cancer-related mortality worldwide (1,2). The poor prognosis of HCC is mainly due diagnosis in later stages, for which there are few effective treatment options. Given that chronic inflammation gives rise to a stromal environment that favors hepatocyte transformation and creates an immunosuppressive milieu that further leads to liver cancer progression, HCCs can be considered a paradigm for inflammation-induced cancers. For this tumor modality, immunotherapy is quite promising (3). Although, there are

© Journal of Gastrointestinal Oncology. All rights reserved.

similar study illustrated the association between genetic and immunological background of HCC and expression of programmed cell death-1 and point out that CD8+ cells were densely infiltrated in PD-L1 positive tumors (4). Thus, there is a pressing need to explore the immune response signaling pathways and the disease microenvironment for HCC initiation and progression.

Immune checkpoint proteins, including PD-1, PD-L1 and CTLA-4, initiate signaling pathways that suppress T-cell function (5). PD-L1, a 40 kDa type I transmembrane protein, is composed of two side-by-side domains and extracellular IgV and IgC domains (6). Despite the approval of targeted inhibitors of sorafenib as first-line treatments for advanced HCC, which could improve survival by several months (7), small molecules of pathway inhibitors may induce drug resistance (8). At present, immune checkpoint inhibitors (ICIs) have shown preferable efficacy in several types of cancer, including lung, breast, bladder, and non-small-cell lung cancers (9-11). In 2017, the US Food and Drug Administration (FDA) approved nivolumab as the first anti-PD-1 antibody for the treatment of HCC. Thus, ICIs might play an indispensable role in HCC treatment, which brings new hope to cancer patients.

PD-L1 is universally expressed both inside and outside of cells (including cancer cells), which can lead to the exhaustion of T cells (12). Some studies have reported that patients with a higher expression of PD-L1 in cancer cells are correlated with preferential outcome in lung cancer (13). However, others have found that a high PD-L1 expression level is a poor prognostic factor in esophageal and cervical cancers (14,15). Although recent studies have been carried out (16-18), the association between the clinical response to anti-PD-1 antibodies and PD–L1 expression in HCC tumor cells remains unclear. Obviously, there is a pressing need to study the features of PD-L1 expression in HCC.

Cancer cells originate from a single cell with accumulated germ-line or somatic mutations and epigenetic alterations, which lead to the transformation of a normal cell into a malignant cell. Existing studies have demonstrated the diversity frequency rates of mutations, such as TP53, CTNNB1, AXIN1, KEAP1, and RB1, in the HCC population (19). The tumor mutational burden (TMB), coupled with PD-L1 expression, has been shown to be a powerful biomarker for ICB selection among different cancer types. The TMB has also been reported to be strongly correlated with the clinical response to immunotherapy using checkpoint inhibitors. Traditionally, the TMB was detected by whole-exome sequencing. However, more recently, targeted gene sequencing (TGS) has been extensively applied in clinical TMB evaluation. Moreover, taking advantage of whole-exome and TGS could provide valuable insight into tumor heterogeneity at the genetic and genomic levels (20).

In this study, we aimed to explore the correlation between PD-L1 expression and the TMB, mutation signature, and driver-gene mutations in 30 Chinese patients with HCC. We also analyzed patient outcomes based on the mutational landscape and the immune microenvironment. Our results highlight the roles of the immune microenvironment and the mutational landscape in patient prognosis, which will help to guide personalized immune-based therapy for Chinese patients with HCC. We present the following article in accordance with the MDAR reporting checklist (available at https://dx.doi.org/10.21037/jgo-21-251).

Methods

Patients and clinical information collection

Thirty-two patients with primary HCC who were admitted to our hospital between May 2019 and November 2020 were included in this study. Written informed consent was obtained from all patients. This study was performed in accordance with the Helsinki Declaration (as revised in 2013) and was approved by the Ethics Committee of the Affiliated Hospital of Guangdong Medical University. Clinical information of the 30 HCC patients were in Table S1.

Hematoxylin-eosin staining and immunohistochemistry

For consensus judgement, all hematoxylin-eosin (HE) images were identified together independently by one otolaryngologist and two experienced pathologists, and the histological subtype classification was assessed according to the World Health Organization's Classification of Tumors [2015]. Formalin-fixed, paraffin-embedded (FFPE) tissue specimens obtained from surgeries were examined in triplicate. Each FFPE tissue was selected from a centrally located area of the tumor that had been confirmed to contain tumor cells by HE staining. FFPE tissue were serial sectioned at a thickness of 4μm and deparaffinized, and then subjected to immunohistochemical staining using a previously described method with a previously validated rabbit monoclonal PD-L1 antibody (E1L3N, 1:800, Cell Signaling Technology, Danvers, MA). For visualization of the antigen, a peroxidase-labeled secondary antibody (DAKO, 22C3) was applied.

© Journal of Gastrointestinal Oncology. All rights reserved.

Table 1 Baseline patient characteristics

Characteristic	Value
Median age in years [range]	58 [34–69]
Gender (male/female)	26/4
Status (alive/dead)	24/6
PD-L1 expression: +/–/NA	10/13/7
Targeted deep sequencing	30
Smoker or ex-smoker/non-smoker	7/23
Never-drinker/ever drinker	18/12
Hepatitis (positive/never)	24/6
CCLC stage (Ia/Ib/IIa/IIb/IIIa)	10/7/7/1/4
BCLC stage (A/B)	12/17
Tumor number (1/2–3/over 3)	19/5/4
Tumor location (SF/C/DC/HF/R)	10/4/5/8/3
Median (range) tumor size, cm	5.5 (1.7–13)
Microvascular invasion (yes/no)	12/18
α-fetoprotein (AFP) >20 μg/L	17

NA, not available; SF, sigmoid flexure; C, cecum; DC, descending colon; HF, hepatic flexure; R, rectum.

DNA extraction

Tumor tissues and matched blood DNA were extracted using the GeneJET FFPE DNA Purification Kit (#K0881, Thermo Scientific, Shanghai, China) according to the manufacturer's instructions. The DNA samples were then identified using the Applied Biological Materials Inc. (ABM), and DNA quality was assessed on Thermo NanoDrop 2000 (Thermo Scientific, Shanghai, China).

Library preparation and sequencing

Genomic DNA were exacted from the tumor tissue sections, and then sonicated into 200 bp fragments in ultrasonic. To prepare the DNA library, we used Roche SeqCap EZ Exome V3 and TruePrep DNA Library Prep Kit V2 for Illumina (#TD501, Vazyme, Nanjing, China) to capture the target DNA, and Illumina HiSeq machines were used to acquire sequencing data. Agilent's SureSelect Human All Exon V5 Kit (Agilent Technologies, Inc. Beijing, China) was applied to capture the whole exome, after amplified modified gDNA fragments in six cycles of PCR. In total, 50 Mb of DNA sequences, containing 33,4378 exons from 20,965 genes, were obtained. The average sequencing depth and coverage of the target region are summarized.

Copy number determination using exome-sequencing data

We aligned bisulfite reads to the reference genome at the candidate locations, and then applied GATA 4.1.4.0 to classify and eliminate PCR duplicates as previously described (21). Copy number variants (CNVs) from the next generation sequencing (NGS) data were calculated by CNVKIT (22). Finally, somatic mutations were converted to MAF and visualized using R package maftools.

Statistical analysis

All clinical and statistical analyses were performed using SPSS version 22.0 (SPSS Inc., Chicago, IL, USA). Clinicopathologic variables of the high and low PD-L1 groups were compared using two-sample t-test or Fisher's exact test for nominal variables. Given that this study was limited to a small sample size, all clinical-related statistical analysis were considered to be significant when $p<0.05$ without multiple correction test.

Results

Patient characteristics

Tumor tissue and blood were collected from 30 patients with HCC at the time of diagnosis. The HCC patients, including 26 males and four females, had an average age of 58 years (range, 34–69 years). Nineteen patients were former smokers, and the remaining 11 were non-smokers. Additionally, 24 male patients and one female patient were never-drinkers, while four male patients were ever-drinkers. Twenty-four patients had hepatitis, while the remaining six patients did not. The number of patients with CCLC stages Ia, Ib, IIa, IIb, and IIIa were 10, seven, seven, one, and four respectively, and the number of those with BCLC stages A and B were 12 and 17, respectively. The exclusion criteria were as follows: (I) patients with prior chemotherapy and radiotherapy, (II) patients with prior non-infectious pneumonitis; and (III) patients with HIV, autoimmune disease, or other conditions that could interfere with their participation in the trial. None of the included patients received radiation therapy previously. The baseline patient characteristics and detailed clinical information are depicted in *Table 1* and Table S1.

© Journal of Gastrointestinal Oncology. All rights reserved.

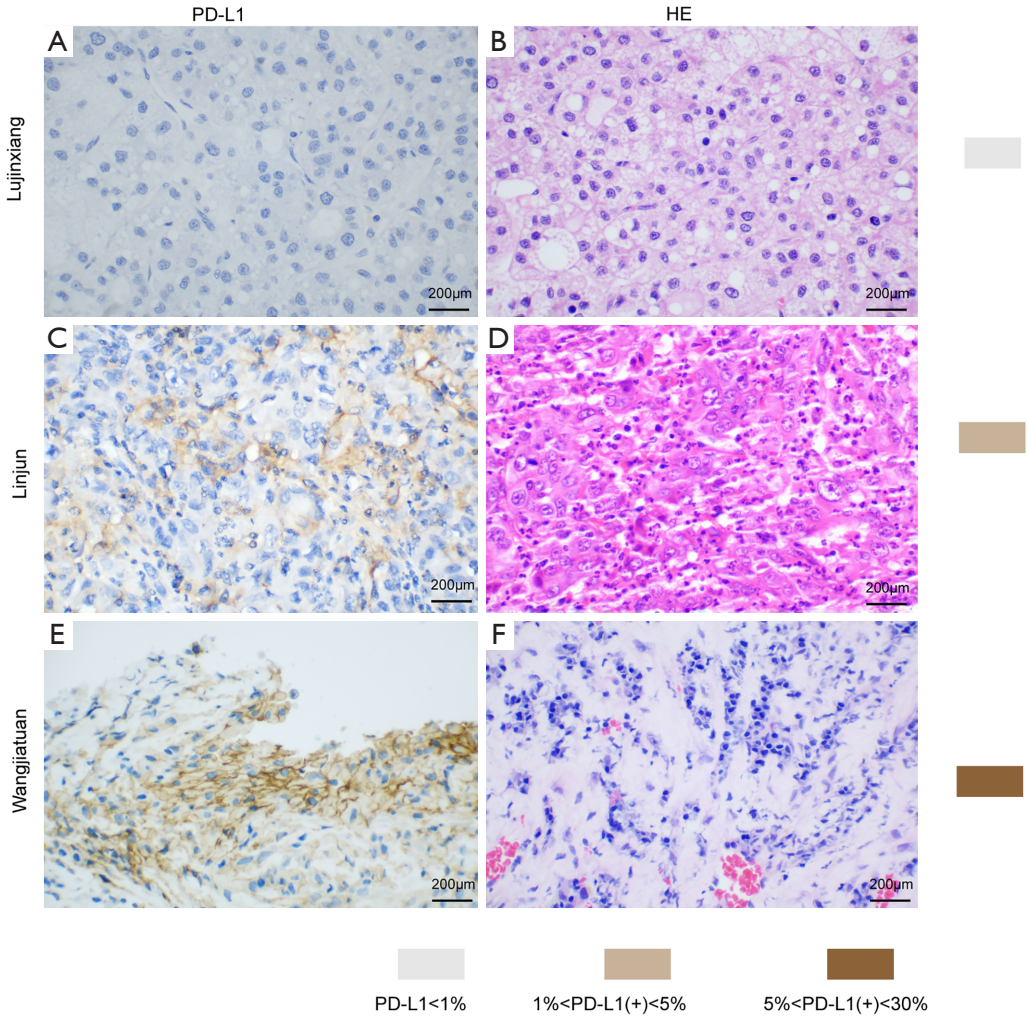

Figure 1 PD-L1 expression in HCC tissue samples. (A) PD-L1 immunohistochemistry of Liujinxiang HCC biopsy. (B) HE staining of Liujinxiang HCC biopsy. (C) PD-L1 immunohistochemistry of Linjun HCC biopsy. (D) HE staining of Linjun HCC biopsy. (E) PD-L1 immunohistochemistry of Wangjiatuan HCC biopsy. (F) HE staining of a representative HCC biopsy. HCC, hepatocellular carcinoma. Scale bars =200 μm.

Correlation between PD-L1 and clinicopathologic features

To evaluate the relationship between PD-L1 and tumor pathological features, we compared the clinicopathologic features with PD-L1 in each tissue sample. Patients were separated into PD-L1 positive and PD-L1 negative groups. We found that the PD-L1 positive patients were more likely to suffer from aggressive clinicopathologic features. These results demonstrate that PD-L1 positive patients possessed more tumors with vascular invasion and advanced CCLC stage (*Figure 1 A*,*B*,*C*,*D*,*E*,*F* and Table S1).

Relationship between PD-L1 and the TMB

The TMB is specified using whole genome sequencing (WGS), whole exome sequencing (WES), or targeted gene panels sequencing. In our study cohort, the PD-L1 positive patients exhibited a lower TMB compared to the PD-L1 negative group. Thus, we may infer that high PD-L1 patients in the Chinese HCC population have a low TMB (*Figure 2*).

Landscape of somatic mutations in HCC patients

To assess somatic alternation, TGS was performed on tissue

© Journal of Gastrointestinal Oncology. All rights reserved.

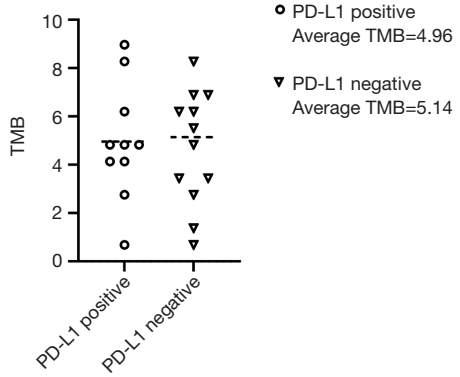

Figure 2 Correlation between PD-1 expression and the TMB. TMB, tumor mutational burden.

samples from the 30 HCC patients. The mean coverage depth for tumor and blood samples was 194×. There were 459 mutation events in 556 genes; the top 30 mutated genes are shown in *Figure 3*. In HCC, the most frequent driver gene mutations were found to be in *TP53*, *CTNNB1*, *KMT2D*, *AXIN1*, *ALK*, and *NOTCH1* (*Figure 3*). The TMB (mutations/Mb) and CNV alteration (CNA) are shown in Table S2.

Mutation spectrum and signatures

Our results revealed that missense mutations were the most common mutation variant cases (*Figure 4A*); and single nucleotide polymorphisms (SNPs) were the most

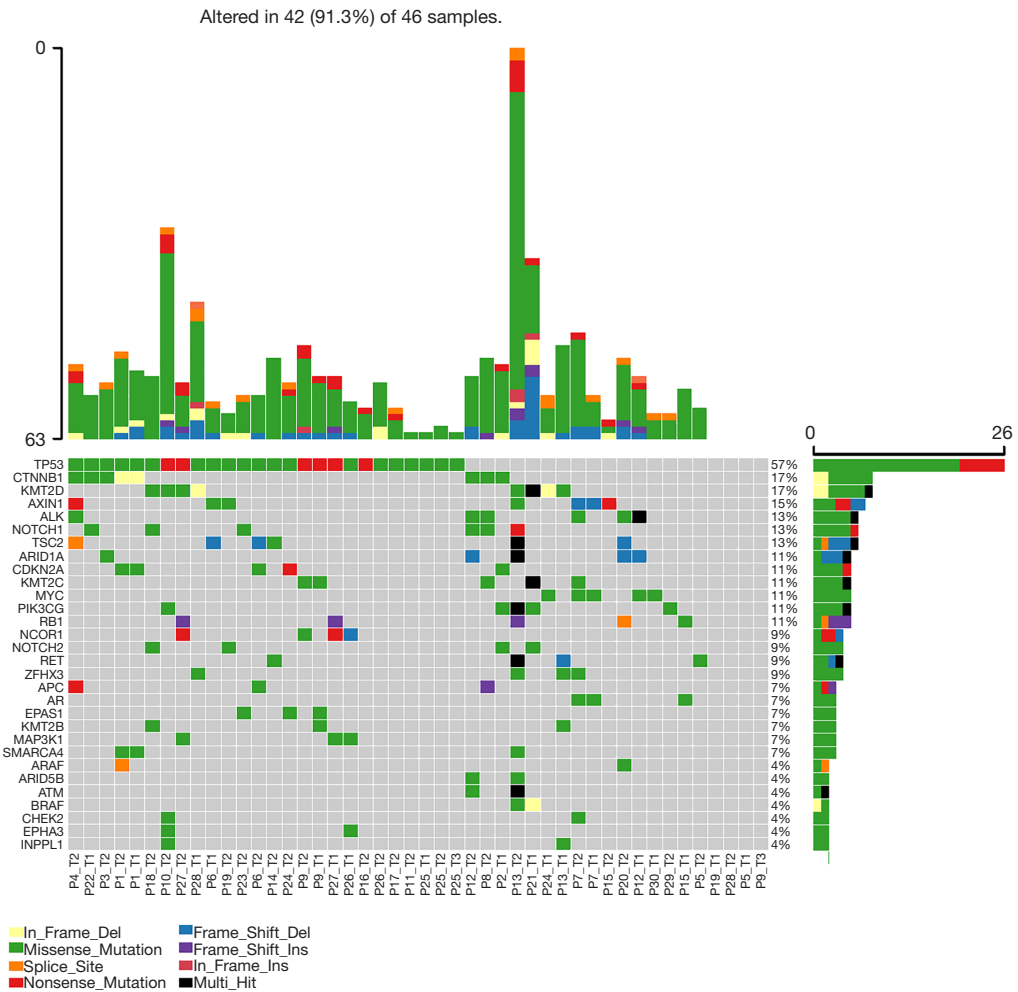

Figure 3 The Oncoprint of the top 30 driver genes in 46 HCC samples. HCC, hepatocellular carcinoma.

© Journal of Gastrointestinal Oncology. All rights reserved.

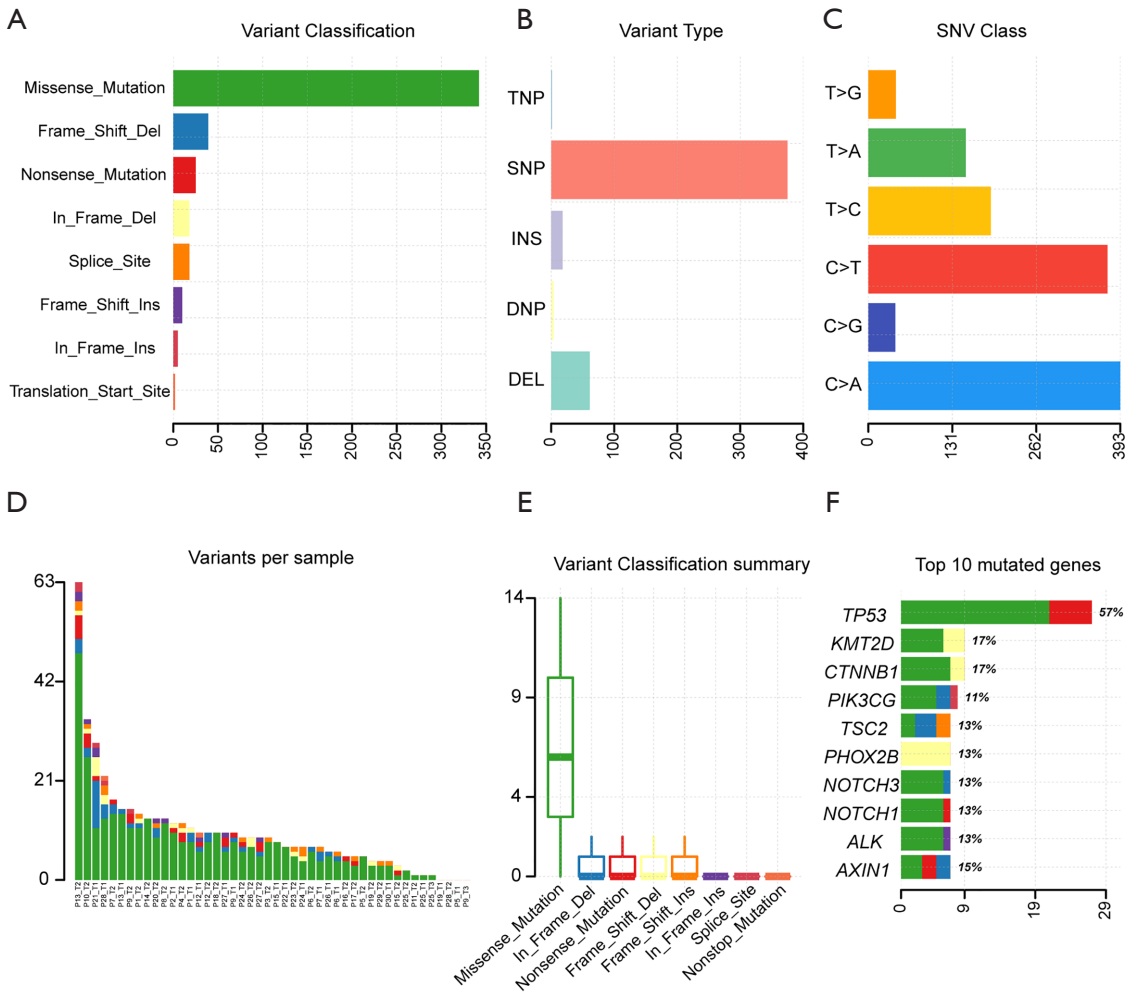

Figure 4 Landscape of somatic mutations of driver genes in HCC. (A) Classification of variant; (B) number of variants; (C) SNV class; (D) number of variants; (D) variants per sample; (E) variant classification summary; (F) top 10 mutated genes. HCC, hepatocellular carcinoma.

common variant types (*Figure 4B*). C > A and C > T were the most common base substitutions (*Figure 4C*); The mean variant of each sample was 9.97, and P13_T2 had the highest mutation number (*Figure 4D*). Variant classification summary also suggested that missense mutations and frame shift deletion was the primarily mutation variant cases (*Figure 4E*). To identify the HCC mutation spectrum and signatures, the top 10 mutated genes in Figure 4F were consistent with SMGs in Figure 5A. Moreover, we identified the significantly mutated genes (SMGs) with $p<0.01$ in the HCC mutation cohort, which included TP53, CTNNB1, AXIN1, TSC2, MST1, RB1, and MYC etc. (*Figure 5A*). We further analyzed mutational signatures 1 and 6 in 46 HCC samples, and found that they were correlated with age of cancer diagnosis and defective DNA mismatch repair, respectively (*Figure 5B*).

Discussion

To demonstrate the genetic mapping of liver cancer, we enrolled 30 Chinese HCC patients (involving 46 HCC tissue samples) in this study. TGS was performed on HCC tumor tissues and matched normal tissues, and their clonal evolution relationships were analyzed. The prevalence of somatic mutations, including nucleotide substitutions, CNA, TMB, and small insertions/deletions, was evaluated by bioinformatics analysis using the R packages, Mutect2 (23,24) and VarDict (25). We also determined the correlation between PD-L1 expression and clinicopathologic features, and TMB. Finally, the landscape

© Journal of Gastrointestinal Oncology. All rights reserved.

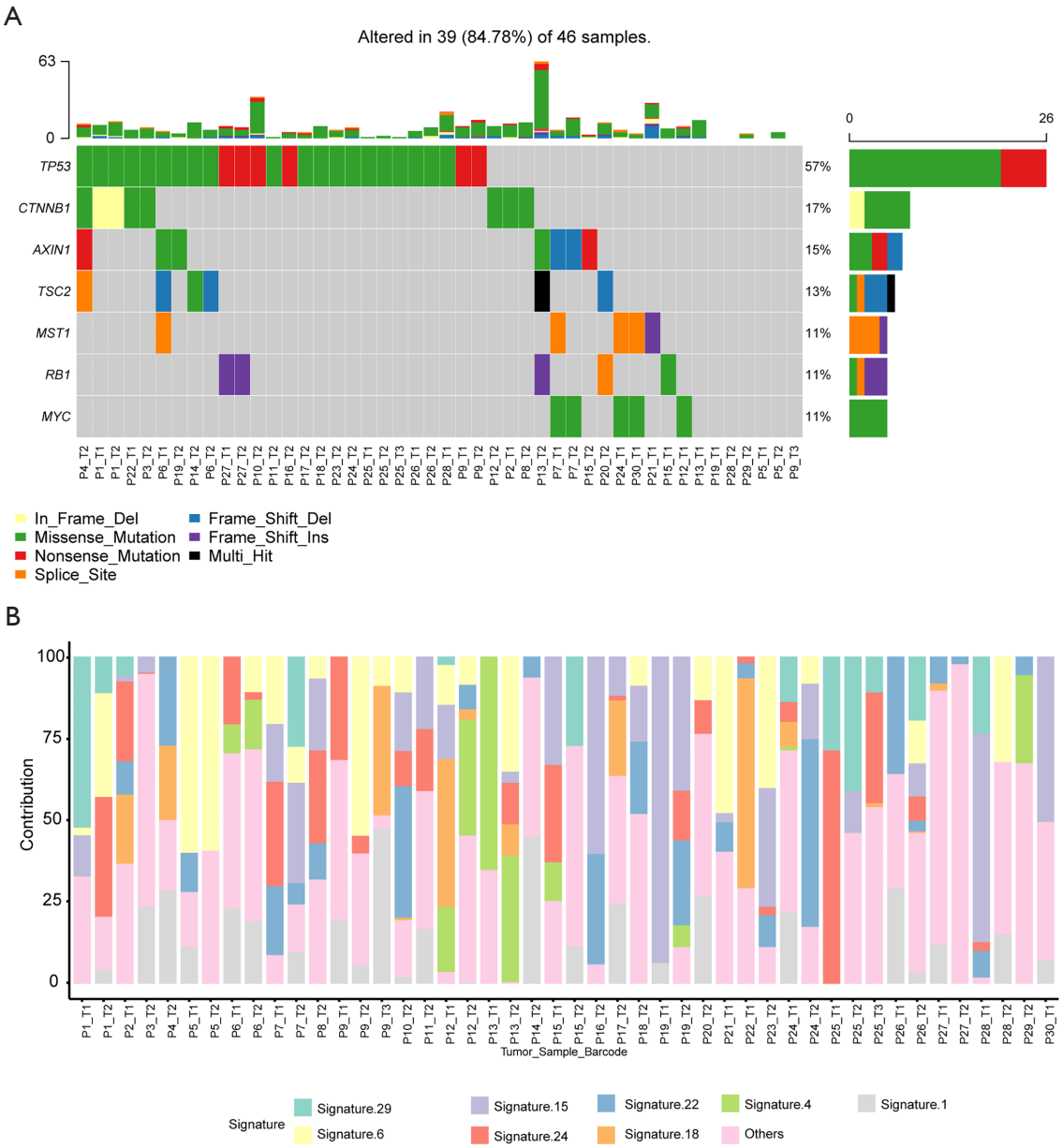

Figure 5 Significant mutated gene and signature distribution. (A) Significant mutated gene of HCC samples; (B) catalogue of somatic mutations of 46 HCC samples according to COSMIC. HCC, hepatocellular carcinoma; COSMIC, Catalogue of Somatic Mutations in Cancer.

of somatic mutations, as well as the mutation spectrum and signatures were calculated as previously described.

Our results suggested that tumors with positive PD-L1 were more likely to suffer from aggressive clinicopathologic features, which is consistent with the results of a previous study (26). Specifically, PD-L1 positive patients possessed more tumors with vascular invasion, and advanced CCLC stage. Moreover, these patients exhibited a lower TMB compared to the PD-L1 negative group. We might speculate that high PD-L1 patients in the Chinese HCC population have a low TMB.

Furthermore, the TMB and overall neoantigen load analysis, as predictors of response to immune checkpoint inhibitors and anti–PD-1 therapy, can alter neoantigen-specific T cell

© Journal of Gastrointestinal Oncology. All rights reserved.

reactivity (27-29). Tumors with high microsatellite instability (MSI-H) accumulate substantial numbers of somatic mutations secondary to deficits in DNA mismatch repair (MMR) (30). The top 30 mutated genes in our dataset indicated that the most frequent driver gene mutations, including *TP53*, *CTNNB1*, *KMT2D*, *AXIN1*, *ALK*, and *NOTCH1*, were consistent with the SMGs, including TP53, CTNNB1, AXIN1, TSC2, MST1, RB1, and MYC etc. However, these results were inconsistent with the findings of Guichard *et al.* (19) and David *et al.* (31) , who reported that the most common driver mutations were in TP53 and CTNNB1.

Missense mutations were the most common mutation variant cases, while C>A and C>T were the most common base substitutions. This is consistent with the findings of Julián *et al.* (31), who described the base substitution differential frequency distribution in HDV+ patients relative to HDV- patients in the Mongolian HCC population. Our results also indicated that SNPs were the most common variant types. The mean variant of each sample was 9.97, and P13_T2 had highest mutation number (63). We further analyzed mutational signatures 1 and 6 in 46 HCC samples, and found that they were correlated with age of cancer diagnosis and defective DNA mismatch repair, respectively.

In this study, we found that the PD-L1 positive HCC patients have a lower TMB than the PD-L1 negative group. It was recommended for PD-L1 positive HCC patients taking anti-PD-1 antibody administration. We also identified the most frequent driver gene mutations in our cohort, including *TP53*, *CTNNB1*, *KMT2D*, *AXIN1*, *ALK*, and *NOTCH1*. This study promotes the potential for PD-L1 inhibitor treatment development for HCC and provides a deep understanding of the HCC mutational landscape, thereby encouraging personalized immune-based therapy for Chinese HCC patients.

Acknowledgments

The authors thank Shanghai Tongshu Biotechnology Co., Ltd. for their technical support.
Funding: None.

Footnote

Reporting Checklist: The authors have completed the MDAR reporting checklist. Available at https://dx.doi.org/10.21037/jgo-21-251

Data Sharing Statement: Available at https://dx.doi.org/10.21037/jgo-21-251

Conflicts of Interest: All authors have completed the ICMJE uniform disclosure form (available at https://dx.doi.org/10.21037/jgo-21-251). The authors report that this work was sponsored by the Shanghai Tongshu Biotechnology Co., Ltd. The authors have no other conflicts of interest to declare.

Ethical Statement: The authors are accountable for all aspects of the work in ensuring that questions related to the accuracy or integrity of any part of the work are appropriately investigated and resolved. This study was performed in accordance with the Helsinki Declaration (as revised in 2013) and was approved by the Ethics Committee of the Affiliated Hospital of Guangdong Medical University. Written informed consent was obtained from all patients.

Open Access Statement: This is an Open Access article distributed in accordance with the Creative Commons Attribution-NonCommercial-NoDerivs 4.0 International License (CC BY-NC-ND 4.0), which permits the non-commercial replication and distribution of the article with the strict proviso that no changes or edits are made and the original work is properly cited (including links to both the formal publication through the relevant DOI and the license). See: https://creativecommons.org/licenses/by-nc-nd/4.0/.

References

1. Llovet JM, Zucman-Rossi J, Pikarsky E, et al. Hepatocellular carcinoma. Nat Rev Dis Primers 2016;2:16018.
2. Ghouri YA, Mian I, Rowe JH. Review of hepatocellular carcinoma: Epidemiology, etiology, and carcinogenesis. J Carcinog 2017;16:1.
3. Heinrich B, Czauderna C, Marquardt JU. Immunotherapy of Hepatocellular Carcinoma. Oncol Res Treat 2018;41:292-7.
4. Nishida N, Sakai K, Morita M, et al. Association between Genetic and Immunological Background of Hepatocellular Carcinoma and Expression of Programmed Cell Death-1. Liver Cancer 2020;9:426-39.
5. Yang K, Li J, Sun Z, et al. Retreatment with immune checkpoint inhibitors in solid tumors: a systematic review. Ther Adv Med Oncol 2020;12:1758835920975353.
6. Dong H, Zhu G, Tamada K, et al. B7-H1, a third member of the B7 family, co-stimulates T-cell proliferation and interleukin-10 secretion. Nat Med 1999;5:1365-9.
7. Zongyi Y, Xiaowu L. Immunotherapy for hepatocellular

© Journal of Gastrointestinal Oncology. All rights reserved.

carcinoma. Cancer Lett 2020;470:8-17.
8. Tyner JW, Tognon CE, Bottomly D, et al. Functional genomic landscape of acute myeloid leukaemia. Nature 2018;562:526-31.
9. Tunger A, Kiessler M, Wehner R, et al. Immune Monitoring of Cancer Patients Prior to and During CTLA-4 or PD-1/PD-L1 Inhibitor Treatment. Biomedicines 2018;6:26.
10. Fan Z, Liang Y, Yang X, et al. A meta-analysis of the efficacy and safety of PD-1/PD-L1 immune checkpoint inhibitors as treatments for metastatic bladder cancer. Onco Targets Ther 2019;12:1791-801.
11. Jing W, Li M, Zhang Y, et al. PD-1/PD-L1 blockades in non-small-cell lung cancer therapy. Onco Targets Ther 2016;9:489-502.
12. Wu Y, Chen W, Xu ZP, et al. PD-L1 Distribution and Perspective for Cancer Immunotherapy-Blockade, Knockdown, or Inhibition. Front Immunol 2019;10:2022.
13. Okita R, Maeda A, Shimizu K, et al. PD-L1 overexpression is partially regulated by EGFR/HER2 signaling and associated with poor prognosis in patients with non-small-cell lung cancer. Cancer Immunol Immunother 2017;66:865-76.
14. Gu X, Dong M, Liu Z, et al. Elevated PD-L1 expression predicts poor survival outcomes in patients with cervical cancer. Cancer Cell Int 2019;19:146.
15. Ito M, Yajima S, Suzuki T, et al. High serum PD-L1 level is a poor prognostic biomarker in surgically treated esophageal cancer. Cancer Med 2020;9:1321-7.
16. Dai X, Pi G, Yang SL, et al. Association of PD-L1 and HIF-1alpha Coexpression with Poor Prognosis in Hepatocellular Carcinoma. Transl Oncol 2018;11:559-66.
17. Huang CY, Wang Y, Luo GY, et al. Relationship Between PD-L1 Expression and CD8+ T-cell Immune Responses in Hepatocellular Carcinoma. J Immunother 2017;40:323-33.
18. Liu CQ, Xu J, Zhou ZG, et al. Expression patterns of programmed death ligand 1 correlate with different microenvironments and patient prognosis in hepatocellular carcinoma. Br J Cancer 2018;119:80-8.
19. Guichard C, Amaddeo G, Imbeaud S, et al. Integrated analysis of somatic mutations and focal copy-number changes identifies key genes and pathways in hepatocellular carcinoma. Nat Genet 2012;44:694-8.
20. Hallou A, Jennings J, Kabla AJ. Tumour heterogeneity promotes collective invasion and cancer metastatic dissemination. R Soc Open Sci 2017;4:161007.
21. Jain A, Chia WK, Toh HC. Immunotherapy for nasopharyngeal cancer-a review. Chin Clin Oncol 2016;5:22.
22. Cao C, Wei Q, Tang X, et al. PD-1 and PD-L1 in locoregionally advanced nasopharyngeal carcinoma: Substudy of a randomized phase III trial. Head Neck 2019;41:1427-33.
23. Liu B, Conroy JM, Morrison CD, et al. Structural variation discovery in the cancer genome using next generation sequencing: computational solutions and perspectives. Oncotarget 2015;6:5477-89.
24. McKenna A, Hanna M, Banks E, et al. The Genome Analysis Toolkit: a MapReduce framework for analyzing next-generation DNA sequencing data. Genome Res 2010;20:1297-303.
25. Lai Z, Markovets A, Ahdesmaki M, et al. VarDict: a novel and versatile variant caller for next-generation sequencing in cancer research. Nucleic Acids Res 2016;44:e108.
26. Gao Q, Wang XY, Qiu SJ, et al. Overexpression of PD-L1 significantly associates with tumor aggressiveness and postoperative recurrence in human hepatocellular carcinoma. Clin Cancer Res 2009;15:971-9.
27. Rizvi NA, Hellmann MD, Snyder A, et al. Cancer immunology. Mutational landscape determines sensitivity to PD-1 blockade in non-small cell lung cancer. Science 2015;348:124-8.
28. S nyder A, Makarov V, Merghoub T, et al. Genetic basis for clinical response to CTLA-4 blockade in melanoma. N Engl J Med 2014;371:2189-99.
29. Van Allen EM, Miao D, Schilling B, et al. Genomic correlates of response to CTLA-4 blockade in metastatic melanoma. Science 2015;350:207-11.
30. Supek F, Lehner B. Differential DNA mismatch repair underlies mutation rate variation across the human genome. Nature 2015;521:81-4.
31. Cancer Genome Atlas Research Network. Electronic address wbe, Cancer Genome Atlas Research N. Comprehensive and Integrative Genomic Characterization of Hepatocellular Carcinoma. Cell 2017;169:1327-41 e23.

(English Language Editor: A. Kassem)

Cite this article as: Xu H, Liang XL, Liu XG, Chen NP. The landscape of PD-L1 expression and somatic mutations in hepatocellular carcinoma. J Gastrointest Oncol 2021;12(3):1132-1140. doi: 10.21037/jgo-21-251

© Journal of Gastrointestinal Oncology. All rights reserved.

Supplementary

Table S1 Clinical information of the 30 HCC patients

Patient	Age	Sex	Smoking	Drinking	BCLC stage	CCLC stage	AFP	Tumor size (cm)	Tumor number	Liver cirrhosis	Hepatitis B	Microvascular invasion	Tumor location	Status
P01	57	M	N	N	B stage	IIa stage	NA	2.4×3.6	1	N	Y	N	DC	Alive
P02	49	M	N	Y	B stage	IIa stage	635.9	6.4×4.8	2-3	Y	Y	Y	SF	Alive
P03	65	M	N	N	B stage	IIa stage	72.9	10.7	2-3	N	Y	N	HF	Alive
P04	60	M	Y	Y	A stage	Ia stage	6.73	3.6×2.8×3.0	1	Y	Y	N	SF	Alive
P05	66	M	N	N	A stage	Ia stage	2676	3.4×3.9	1	Y	Y	N	C	Alive
P06	63	F	N	N	A stage	Ib stage	5172	6.3×5.2	1	Y	Y	N	SF	Alive
P07	63	M	N	Y	A stage	Ib stage	6.82	6.0×5.0×6.0	1	Y	N	N	C	Dead
P08	47	M	Y	N	B stage	IIa stage	15.41	2.5×2.0×2.4	>3	N	N	Y	HF	Alive
P09	46	M	N	N	B stage	IIa stage	3.77	10.1×9.2×9	2-3	N	Y	N	SF	Alive
P10	58	F	N	Y	A stage	IIa stage	551.40	4.3×4.0×3.5	2-3	Y	Y	N	DC	Alive
P11	67	M	N	Y	B stage	Ia stage	3846	4.4×3.5	1	Y	Y	N	SF	Alive
P12	65	F	Y	N	B stage	Ib stage	9.15	7.2×10.2×12	1	N	N	N	SF	Alive
P13	63	M	Y	N	A stage	Ib stage	NA	1.7×10.2×1	2-3	Y	Y	N	R	Dead
P14	54	M	N	N	A stage	Ia stage	883.6	3.2×3.1×3.9	1	Y	N	N	HF	Alive
P15	64	M	N	Y	B stage	IIb stage	582.2	2.0×2.0×2.0	Diffusion	Y	Y	Y	SF	Alive
P16	51	M	N	Y	B stage	Ia stage	37,404	9.2×6.0×7.9	1	N	Y	Y	R	Dead
P17	52	M	Y	N	B stage	IIIa stage	78,487	10×7.3×8.4	>3	N	Y	N	DC	Alive
P18	48	M	N	Y	B stage	Ib stage	2,879	10×12×11	1	Y	Y	Y	HF	Alive
P19	45	M	N	N	NA	NA	4.7	NA	1	N	Y	N	SF	Alive
P20	54	M	N	N	B stage	IIIa stage	3.6	8.6×7.1×10	>3	Y	Y	Y	HF	Dead
P21	44	M	N	N	A stage	Ia stage	1,438	4.3×3.6×4.0	1	Y	Y	N	DC	Alive
P22	34	M	N	N	A stage	Ia stage	4.98	1.7×1.3	1	N	Y	Y	C	Alive
P23	59	M	Y	Y	A stage	Ia stage	5.55	4.8×4.2×4.8	1	N	Y	N	SF	Alive
P24	51	M	N	Y	B stage	IIIa stage	44.47	4.5×4.2×3.9	>3	N	Y	Y	HF	Alive
P25	69	M	N	N	B stage	IIIa stage	600	6.0×5.2×6.0	1	N	Y	Y	DC	Dead
P26	47	F	N	Y	A stage	Ia stage	45.64	2.0×1.5×1.6	1	N	Y	N	SF	Alive
P27	58	M	Y	N	A stage	Ia stage	5.44	1.8×2.2×2.2	1	Y	Y	N	C	Alive
P28	61	M	N	Y	B stage	Ib stage	25,399	13×9.3×10	1	N	N	Y	HF	Alive
P29	68	M	N	N	B stage	Ib stage	75.69	7.0×6.6×6.5	1	Y	Y	N	HF	Alive
P30	57	M	N	N	B stage	IIa stage	NA	NA	NA	Y	Y	N	R	Dead

HCC, hepatocellular carcinoma; NA, not available; SF, sigmoid flexure; C, cecum; DC, descending colon; HF, hepatic flexure; R, rectum.

© Journal of Gastrointestinal Oncology. All rights reserved.
https://dx.doi.org/10.21037/jgo-21-251

Table S2 Statistical information of variant and classification summary

ID	Variants	TMB	CNA_burden	wGII	ITH	SDI
P1_T1	11	7.587886698	22.75258576	0.415428647	3	0.73562194
P1_T2	14	9.657310342	92.43735571	0.803299206	2	0.636514168
P10_T2	34	23.45346797	89.70924974	0.376814385	6	1.386956371
P11_T2	1	0.689807882	5.381965054	0.909090909	2	0.666278442
P12_T1	10	6.898078816	15.09639084	0.863636364	2	0.295439192
P12_T2	10	6.898078816	92.00613737	0.658218235	1	0
P13_T1	15	10.34711822	0.154996755	0.274063861	3	0.212626824
P13_T2	63	43.45789654	53.23273409	0.727272727	4	0.534053922
P14_T2	13	8.967502461	0	0.590909091	3	0.907808692
P15_T1	8	5.518463053	4.963319722	0.545454545	2	0.202273002
P15_T2	3	2.069423645	8.27205916	0.258685651	3	0.923840706
P16_T2	5	3.449039408	0.818896847	0.545454545	1	0
P17_T2	5	3.449039408	0.076048791	0.909238851	2	0.693147181
P18_T2	10	6.898078816	9.867542383	1	2	0.661563238
P19_T1	0	0	6.55921377	0.467909025	1	0
P19_T2	4	2.759231526	7.479571355	0.97091043	2	0.579915171
P2_T1	12	8.277694579	0.343328663	0.369047515	4	0.939025933
P20_T2	13	8.967502461	37.57842333	1	2	0.376770161
P21_T1	29	20.00442857	0	0.181818182	2	0.286835983
P22_T1	7	4.828655171	26.64599302	1	1	0
P23_T2	7	4.828655171	27.8832033	0.408533033	2	0.562335145
P24_T1	7	4.828655171	0.002361299	0.090909091	2	0.636514168
P24_T2	9	6.208270934	19.71947899	0.397509469	2	0.636514168
P25_T1	1	0.689807882	0.471641359	0.303252167	1	0
P25_T2	2	1.379615763	64.76620467	0.590414607	1	0
P25_T3	1	0.689807882	0.154184895	0.409090909	1	0
P26_T1	6	4.13884729	0.417709133	0.727272727	4	1.308605387
P26_T2	9	6.208270934	0	0.045454545	2	0.636514168
P27_T1	10	6.898078816	26.00566056	0.673307614	3	0.907535294
P27_T2	9	6.208270934	2.069159892	0.365414961	1	0
P28_T1	22	15.1757734	11.14034432	0.56751439	2	0.15841057
P28_T2	0	0	0.886233424	0.473588193	1	0
P29_T2	4	2.759231526	40.23725906	0.84470306	3	0.979971182
P3_T2	9	6.208270934	33.80397322	0.65037642	2	0.686961577
P30_T1	4	2.759231526	38.60695234	0.818181818	2	0.636514168
P4_T2	12	8.277694579	51.32442012	1	1	0
P5_T1	0	0	4.389571242	0.818181818	1	0
P5_T2	5	3.449039408	2.260930815	0.403865147	1	0
P6_T1	6	4.13884729	2.956001221	0.784427944	1	0
P6_T2	7	4.828655171	13.25366971	0.361996109	2	0.429323022
P7_T1	7	4.828655171	0.002369745	0.363636364	1	0
P7_T2	17	11.72673399	25.75794218	0.454545455	2	0.462036909
P8_T2	13	8.967502461	5.695953604	1	3	1.026330633
P9_T1	10	6.898078816	1.853768256	0.954545455	2	0.590842246
P9_T2	15	10.34711822	86.3420099	0.954545455	3	0.848685558
P9_T3	0	0	0.25404093	0.093301692	1	0

GII, genomic instability index; ITH, intra-tumor heterogeneity; SDI, shannon diversity index.

© Journal of Gastrointestinal Oncology. All rights reserved.
https://dx.doi.org/10.21037/jgo-21-251